Composites Part B 142 (2018) 241–250

Contents lists available at ScienceDirect

Composites Part B

journal homepage: www.elsevier.com/locate/compositesb

Recent advances in carbon-fiber-reinforced thermoplastic composites: A review

Shan-Shan Yao[a], Fan-Long Jin[a], Kyong Yop Rhee[b,*], David Hui[c], Soo-Jin Park[d,**]

[a] Department of Polymer Materials, Jilin Institute of Chemical Technology, Jilin City 132022, People's Republic of China
[b] Department of Mechanical Engineering, College of Engineering, Kyung Hee University, Yongin 446-701, Republic of Korea
[c] Department of Mechanical Engineering, University of New Orleans, LA 70148, United States
[d] Department of Chemistry, Inha University, Incheon 402-751, South Korea

ARTICLE INFO

Keywords:
Carbon fiber
Thermoplastic resin
Electrical properties
Mechanical properties

ABSTRACT

Carbon fibers (CFs) have high specific tensile strength, high modulus, and outstanding wear resistance, and are widely used for the reinforcement of advanced composite materials. CF-reinforced thermoplastic composites have received much attention because of their easy processability and recycling convenience compared with thermosetting composites. Surface treatment of CFs is generally employed to increase the surface functional groups and interfacial adhesion between the CFs and the surrounding polymer matrix. In this review, we explore recent advances in the surface treatment of CFs and preparation of CF/thermoplastic composites. The thermal, mechanical, and electrical properties of the composites are also discussed.

1. Introduction

Carbon fibers (CFs) have been widely used to reinforce advanced composite materials because of their exceptional properties, such as high specific tensile strength, high modulus, and outstanding wear resistance. CFs can be classified as continuous CFs, long CFs, and short CFs (SCFs) based on the length of the fiber. CF-reinforced polymers exhibit outstanding mechanical properties and low density and are widely used in the fields of aerospace, transportation, and sporting goods [1–10].

In CF-reinforced composites, the polymer usually acts as the continuous phase (the matrix), and the CF serves as the discontinuous phase. The polymer matrices can be classified into thermosetting and thermoplastic resins. Thermoplastics can be further divided into general plastics, such as polyethylene (PE), polypropylene (PP), and acrylonitrile butadiene styrene (ABS) resins, and engineering plastics, such as polyamide (PA), polycarbonate (PC), polyetheretherketone (PEEK), polyetherimide (PEI), polyethersulfone (PES), and polyphenylene sulfide (PPS). Thermoplastics have received significant attention as polymer matrices because of their lack of requirement for a curing stage and their less hazardous chemical compositions and improved recycling convenience and mass production capability compared with conventional thermosetting resins. Thermoplastic resins are often fabricated using conventional molding methods, such as injection–molding, rotational–molding, extrusion, vacuum forming, and compression–molding [11–19].

However, the surface of pristine CFs is non-polar, whereas, the polymer matrix generally exhibits polar character. The strength of the interfacial bonds between the CFs and matrix is consequently poor, thereby precluding achievement of the ideal mechanical properties of the composites. Thus, numerous CF surface treatment methods, such as wet chemical or electrochemical oxidation, ozone treatment, polymer or metal coating, and plasma treatment, have been proposed to increase the surface functional groups and interfacial adhesion between the CFs and surrounding polymer matrix [20–28].

In this report, various methods for surface treatment of CFs and the preparation of CF-reinforced thermoplastic composites are reviewed in detail. In addition, the thermal, mechanical, and electrical properties of the composites are discussed.

2. Surface treatment of CFs

Zhang et al. [29] treated CFs with a mixture of concentrated sulfuric/nitric acid in a reaction flask. The flask was placed in an ultrasonic water bath to maintain the treatment temperature. The treated CFs were washed several times with distilled water. Wu et al. [30] also treated CFs with nitric acid at 115 °C for 20–90 min. The CFs were then refluxed with 1.0 N NaOH solution, extracted with distilled water, and

* Corresponding author.
** Corresponding author.
E-mail addresses: rheeky@khu.ac.kr (K.Y. Rhee), sjpark@inha.ac.kr (S.-J. Park).

https://doi.org/10.1016/j.compositesb.2017.12.007
Received 3 July 2017; Received in revised form 6 November 2017; Accepted 15 December 2017
Available online 16 December 2017
1359-8368/

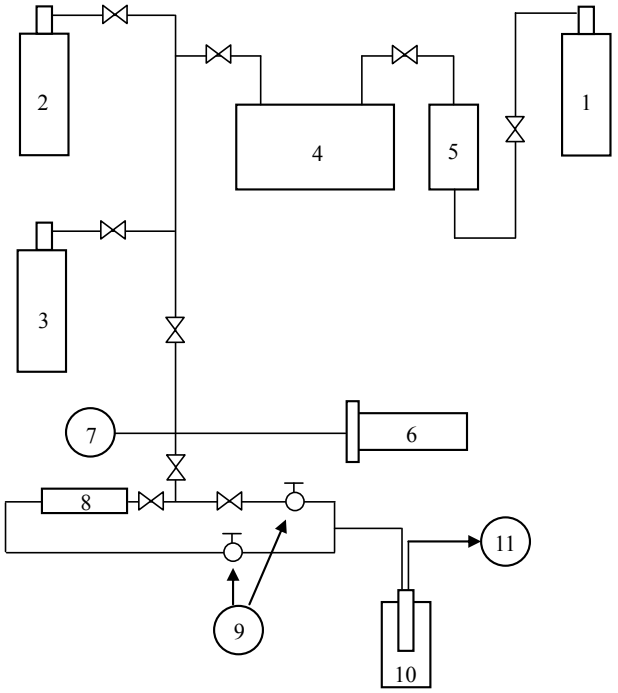

Fig. 1. Schematic diagram of fluorination reactor [27]. 1: F_2 gas cylinder, 2: N_2 gas cylinder, 3: O_2 gas cylinder, 4: Buffer tank, 5: HF absorber, 6: reactor, 7: pressure gauge, 8: F_2 absorber, 9: glass cock, 10: liquid nitrogen, 11: rotary vacuum pump.

dried in ambient air. Their results indicated that oxidation by nitric acid effectively generated significant amounts of acidic functional groups on the surfaces of CFs. Ryu et al. [31] treated CFs with aqueous ammonium carbonate solution using an original continuous treatment process. The length of the electrolytic treatment bath was 0.23 m, and the total oxidized fiber surface area was 0.032 m^2. X-ray photoelectron spectroscopic (XPS) analysis indicated that the O_{1s}/C_{1s} and N_{1s}/C_{1s} ratios of the treated CFs increased with increasing current intensity.

Park et al. [27,32–35] investigated the effect of oxyfluorination on the surface characteristics of CFs. The oxyfluorination reaction was performed in a batch reactor, as shown in Fig. 1. The fluorine and oxygen mixtures were introduced into the reactor at room temperature and the reactor was then heated to the treatment temperature. After the reaction, the specimens were cooled and the reactor was purged with nitrogen. Fourier-transform infrared (FT-IR) analysis indicated that the oxyfluorinated CFs contained carboxyl/ester and hydroxyl groups and the –O–H peak was more intense than that of the fluorinated counterparts. Park et al. [36] also studied the effect of anodic oxidation of CFs on the fracture toughness of CF-reinforced epoxy composites. Electrochemical treatment of the CFs was conducted using a laboratory pilot-scale apparatus, as shown in Fig. 2. The electrolyte was a 10 wt% phosphoric acid solution. After anodic oxidation, the CFs were washed with distilled water and then rinsed by immersion in acetone for 2 h. Contact angle measurements indicated that anodic oxidation led to an increase in the surface free energy, mainly by increasing the polar component. Park et al. [37] further proposed an interpretation based on more precise linear free energy relationships for describing the acid − base interaction at a solid surface. The CFs were subjected to anodic treatment at an oxidation voltage of 1.6 V on a pilot scale. Electrochemical treatment of the CFs significantly improved the acid − base character.

Osbeck et al. [38] investigated the effect of ultraviolet-generated ozone treatment on the surface functionality and structure of CFs. The CFs were electrochemically treated in a base oxidation bath prior to further photosensitized oxidation in a UVO cleaner/oxidizer. XPS analysis indicated that functional groups such as hydroxyl species, alkoxides, carbonyl, and carboxyl groups were introduced in the ozone-treated CFs. Park et al. [39] also studied the gas − phase ozone treatment of CFs for introducing acidic oxygen functional groups onto the surfaces of CFs. Ozone treatment of the CFs was performed at ozone concentrations in the range of 10–40 mg/l at room temperature. FT-IR and XPS analyses indicated that oxygen functional groups, such as −OH, O − C = O, C = O, and C − O, were attached to the surfaces of the CFs after the ozone treatment.

Zhang et al. [40] treated CFs using an oxidation–reduction method followed by coating with vinyl silsesquioxane (VMS–SSO) to improve the interfacial properties of CF/polyarylacetylene (PAA) composites. The oxygen plasma treatment was performed in a plasma processor. The CFs were reduced with $LiAlH_4$/THF saturated solution and then coated with VMS–SSO. The XPS results indicated that the number of polar functional groups increased after the redox reaction. The VMS–SSO coating treatment introduced vinyl groups, which could react with the PAA resin during the PAA curing process. Iwashita et al. [41] studied the treatment of CFs using either silane or titanate coupling agents. A CF bundle was immersed in a solution containing 1 wt% coupling agent and then dried in air at 120 °C for 30 min. The tensile strength of the carbonized composite was improved by both coupling treatments.

Park et al. [42] prepared a Ni–P coating on the surfaces of CFs to improve the impact resistance of CF–reinforced epoxy composites. The CFs were activated in nitric acid for 30 min and then sequentially activated in tin chloride and palladium chloride solutions. Nickel-plated CFs were obtained by dipping the CFs in a nickel bath, washing with distilled water, and drying in a vacuum oven at 120 °C for 12 h. X-ray diffraction (XRD) and XPS analyses indicated that Ni–P coating of the CFs led to an increase in the microcrystalline and amorphous phases. Park et al. [21,43–45] also performed electrolytic plating of metallic nickel on the surface of CFs to improve the interfacial adhesion and mechanical properties of CF/phenolic matrix composites. The CFs were activated in nitric acid, tin chloride, and palladium chloride solutions. Nickel-plated CFs were obtained by dipping the CFs in a nickel bath. The oxygen functional groups and metallic nickel on the CF surfaces were found to greatly affect the mechanical interfacial behavior of the composites.

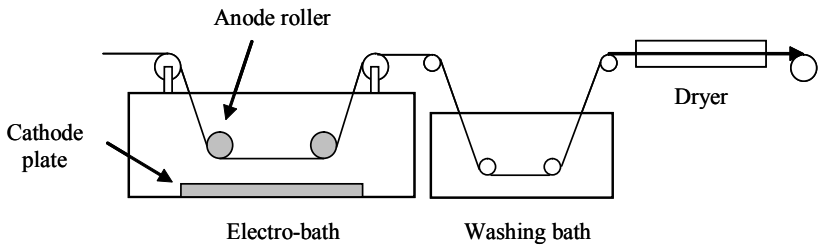

Fig. 2. Schematic representation of continuous electrolytic surface anodization process [36].

3. Sample preparation

3.1. ABS-based composites

3.1.1. Preparation method I

ABS resin was mixed with chloroform to form a paste; the desired amount of CFs was dispersed in the paste by mechanical stirring. The CF-filled paste was dried at room temperature and then molded by hot pressing at 200–210 °C for 5 min [46,47].

3.1.2. Preparation method II

The desired amount of CFs was chopped into 5 − mm pieces and mixed with ABS resin in a Brabender mixer operating at 210 °C for 3 min. The mixture was then hot compression − molded at 200–210 °C for 5 min [46,48].

3.1.3. Preparation method III

A twin-screw extruder was preheated for 2 h and ABS was then used to clean the extruder for 10–15 min. The CF/ABS mixture was loaded into the machine at 260 °C using a rolling speed of 110 rpm. The CF/ABS mixture was hot compression − molded at 240 °C and 150 kg/cm^2 for 4 min [49–51].

3.2. PA-based composites

3.2.1. Preparation method I

PA was mechanically mixed with CFs and then extruded using a twin-screw extruder in the temperature range of 190–230 °C at a rotational speed of 20 rpm. The extrudate was pelletized, dried, and injection − molded into standard test samples [52,53].

3.2.2. Preparation method II

SCF-reinforced PA composites were prepared by melt mixing at 240 °C for 3 min using a laboratory-scale co-rotating twin-screw mini extruder. The compounds were subsequently injection − molded using a laboratory-scale injection − molding machine using a barrel temperature of 240 °C, mold temperature of 30 °C, and injection pressure of 8 bar [54–57].

3.2.3. Preparation method III

The CFs and solvent (1:5 wt/wt) were mixed and the mixture was treated by ultrasonic oscillation at 30 °C for 2 h. The PA pellets, solvent, CF suspension, and lubricant were combined in a reactor, stirred at 145 °C for 2–3 h, and then cooled to 105 °C. After distillation of the solvent, the precipitate was vacuum-dried and ball-milled. The CF/PA composite powders were thus obtained [58].

3.2.4. Preparation method IV

Unidirectional laminates with CFs and PAs were manufactured using a steel mold. The laminates with 40 vol% CF were obtained by sequentially winding CF cables over the PA sheets by alternatively stacking five PA sheets and five unidirectional CF layers. The two winding unidirectional prepregs were consolidated using hot compression − molding [59].

3.2.5. Preparation method V

Dried PA pellets were melted and forced to pass through a heated impregnation die using a single screw extruder at 230 °C. CF tows in the spool were pulled through the same die, where the CF tows were coated with a layer of PA, forming core/shell structured composite wire rods. The composite wire rods were cooled and chopped into core/shell-structured pellets [60].

3.2.6. Preparation method VI

Continuous CF-reinforced PA composites were prepared using a 3D printing system. The PA matrix was firstly printed and the continuous fiber reinforcement was then printed. The PA and fiber layers were printed onto a print bed using a hot end temperature of 263 °C [61].

3.2.7. Preparation method VII

Continuous − CF-reinforced PA 6 composites were prepared using a melt impregnation method by passing fiber bundles through a crosshead impregnation die. The volume fraction of the fiber was controlled in the range of 50.0 ± 2.0% and the thickness and width were 0.25 ± 0.03 mm and 7.00 ± 0.15 mm, respectively [62].

3.3. PC-based composites

3.3.1. Preparation method I

PC pellets were completely dissolved in tetrahydrofuran (THF). SCFs were dispersed in THF using a stirring and sonification process. The PC solution was added to the CF mixture. The mixture was sonicated and stirred for 15 min before being cast into a mold, and placed in a furnace at 50 °C for 7 min. Finally, the sheets were compacted at 180 °C and 25 kN for 10 min using a hot compress machine [63].

3.3.2. Preparation method II

SCF/PC composites were prepared at 300 °C by compounding with a twin-screw extruder for 1 h. The solid was compacted by a hot compressor at 180 °C and 25 kN for 20 min. The material was placed in a furnace at a temperature above the glass transition temperature (T_g) of PC [64,65].

3.3.3. Preparation method III

SCF-reinforced PC composites were prepared by treatment of the components in a micro-compounder at 295 °C for 3 min, followed by molding using an injection molding machine with a barrel temperature of 295 °C, mold temperature of 100 °C, and injection pressure of 10 bar [66].

3.4. PEEK-based composites

3.4.1. Preparation method I

Unidirectional composite specimens with fiber orientations of 0° and 90° were prepared by hot pressing CF/PEEK prepregs into unidirectional laminates and then cutting the laminates into specimens [67,68].

3.4.2. Preparation method II

The compounding of PEEK with CFs was achieved using a twin-screw extruder at 360–390 °C; a screw speed of 360 rpm and feed rate of 18 rpm were employed. The extrudate was continuously cooled in water and pelletized. Standard test bars were injection − molded at 180 °C [69].

3.4.3. Preparation method III

In this method, 30 wt% SCF-containing PEEK composites were prepared at processing temperatures of 360–390 °C using an injection − molding machine [70].

3.4.4. Preparation method IV

CFs and PEEK powder were dispersed in alcohol using a ball grinder. The mixture was dried at 90 °C for 24 h. The CF/PEEK composites were produced at 380 °C using an injection-molding machine. The resulting composite was injected into molds [71].

3.4.5. Preparation method V

Continuous CF-reinforced PEEK composite cylinders comprising a PEEK matrix, continuous CF, and internal lubricants, were produced by a filament winding process [72].

3.4.6. Preparation method VI

Unidirectional laminated long CF/PEEK composite plates were prepared by compression – molding. The micro-braided yarn was unidirectionally wound around a stainless-steel frame with adequate tension. The frame was then placed in a mold that was put on the platform of a hot press machine and subjected to programmed heating and pressure [73].

3.5. PEI-based composites

3.5.1. Preparation method I

Unidirectional CF tapes were clamped on a frame, followed by application of layers of a viscous solution of PEI in dichloromethane using a hand layup technique. Two unidirectional strokes of coats were applied and then dried under ambient environment. These dried prepregs were then compression – molded at 390 °C and 32 kN/m^2 for 20 min [74,75].

3.5.2. Preparation method II

SCF-reinforced PEI composites were prepared using a twin-screw extruder. The screw temperature and rotation speed were 385 °C and 10 rpm, respectively. The extrudate was molded into a rectangular plate by compression – molding [76].

3.5.3. Preparation method III

PEI was dissolved in a mixture solvent, and continuous CF bundles were impregnated into the PEI solution. The solution-processed prepreg was allowed to dry on the drum and then vacuum-oven treated at 100–200 °C for 10 h. The prepreg was laid up and compressed into unidirectional composite panels using a hot-press molding method [77].

3.6. PES-based composites

3.6.1. Preparation method I

PES films were pre-cut to the cavity dimensions and placed in the mold. A single CF was placed on the stack of PES films. Both ends of the CF were fixed to the mold with polyimide adhesive tape. Additional PES films were placed on top of the CF. The mold was heated in a pressclave at 300 °C for 30 min and then slowly cooled to room temperature [78].

3.6.2. Preparation method II

PES was dissolved in a mixture solvent, and continuous CF bundles were impregnated into the PES solution. The solution-processed prepreg was dried and treated at 100 – 200 °C for 10 h. The prepreg was laid up and compressed into unidirectional composite panels using a hot-press molding method [77,79,80].

3.6.3. Preparation method III

SCF/PES composites were prepared using a co-rotating twin-screw extruder. The temperature of the barrel was in the range of 360–375 °C. The extrudates were continuously cooled and pelletized. Standard test bars were obtained by injection – molding at 180 °C using a plastic-injection molding machine [81].

3.6.4. Preparation method IV

Unidirectional composites were fabricated with poly(phthalazinone ether sulfone ketone) (PPESK)/PES blends as the matrix and continuous CF as the reinforcement. Continuous CF bundles were impregnated into the polymer solution. The individual bundles were wound on – to a stainless – steel plate. The solution-processed prepreg was allowed to dry on the drum and then treated at 100–200 °C for 10 h [77].

3.7. PE-based composites

3.7.1. Preparation method I

The PE and CFs were mixed at 190 °C for 10 min using a two-roll mill. The mixture was melted by treatment at 190 °C for 10 min and compressed under a pressure of 18 MPa for 15 min, followed by quenching in water to obtain the films [82–85].

3.7.2. Preparation method II

PE, CFs, and compatibilizers were mixed using a co-rotating twin screw extruder at 50–210 °C and 100 rpm. The extrudate was pelletized and molded using a laboratory-scale injection-molding machine at a barrel temperature of 200 °C and mold temperature of 30 °C [86].

3.7.3. Preparation method III

Several layers of a cross-plied-woven roving CF mat were positioned individually on aluminum foil, and powdered high-density polyethylene (HDPE) was spread on these layers. The layers were placed on one another and enfolded in aluminum foil. The stacked laminate was placed between the platens of a high-temperature hydraulic press at 140 °C and compressed at 2500 psi for 2 h [87].

3.8. PPS-based composites

3.8.1. Preparation method I

PPS resin was melted and pulled into CFs and then knotted loosely around a CF monofilament. The sample was placed onto a microscope melting point apparatus at 300 °C and kept for 1 min; the specimen was then removed from the hot plate and cooled to ambient temperature. The prepared samples were annealed at 120 °C for 12 h [88].

3.8.2. Preparation method II

PPS and CFs were compounded using a mini-twin-screw extruder at 230 °C for 10 min. The melted composites were continuously injected into the mold at an injection temperature of 250 °C [89–91].

3.9. PP-based composites

3.9.1. Preparation method I

CFs and PP particles were mixed together in a mortar. The mixture was subjected to strong mechanical stirring in ethanol for 1 h and ultrasonication for another 1 h. After complete evaporation of the ethanol, the mixture was compression – molded into sheets at 190 °C under a pressure of 15 MPa [92,93].

3.9.2. Preparation method II

PP and SCF were compounded using a co-rotating twin-screw mini-extruder at 230 °C. The compounds were subsequently injection – molded using an injection – molding machine employing a barrel temperature of 230 °C, mold temperature of 25 °C, and injection pressure of 8 bar [94,95].

3.9.3. Preparation method III

CF/PP composites were prepared by melt-blending PP with CFs. The mixed samples were compressed under a pressure of 7.5 MPa at 200 °C for 20 min using a hot press. The mold was cooled to room temperature using a cooling system [96,97].

3.9.4. Preparation method IV

PP resins and coupling agents were mixed in a single screw extruder. Long roving type CFs were impregnated into the PP die. The composite of PP impregnated with long CFs was water-cooled, pelletized with 10 mm pellets, and dried [98].

3.9.5. Preparation method V

Unidirectional and quasi-isotropic preconsolidated laminates were

heated to the melting temperature of PP and then stamp－formed in a cold－matched metal tool. A continuous CF-reinforced PP prepreg with approximately 20% fiber was used. The prepreg sheet had a thickness of 0.4–0.5 mm [99].

4. Thermal, mechanical, and electrical properties

4.1. ABS-based composites

Li et al. [51,100] studied the tensile properties of HNO_3-treated SCF/PA6/ABS composites. Their results indicated that the tensile strength and tensile modulus of the composites improved when the SCF content was increased from 10 wt% to 30 wt%. The tensile properties of the composites were also enhanced by increasing the PA6 content due to improved interfacial adhesion.

Lu et al. [46] investigated the electrical conductivity and shielding effectiveness of CF/ABS composites. The resistivity of the nickel-coated CF/ABS composites decreased with an increase in the CF content. For the same CF content, the conductivity of the composites with nickel-coated CFs was much greater than that of the non-coated composites. The shielding effectiveness of ABS resin filled with 10 vol% of nickel-coated CFs was 50 dB. Liang et al. [47] also investigated the resistivity of SCF/ABS resin composites. The composites displayed good conductivity when the SCF content was greater than 2 vol%. The resistivity of the composites decreased with increasing SCF length and surface treatment of the SCFs.

Tzeng et al. [48] studied the electromagnetic interference (EMI) shielding effectiveness of copper- and nickel-coated CF-reinforced ABS composites. Their results indicated that the electroless-nickel-coated CF/ABS composites exhibited the best EMI shielding capability because of the longer fiber length distribution and excellent bonding between the nickel coating and fibers. Huang et al. [50] also investigated the EMI shielding effectiveness of CF/PC/ABS composites. Nickel-coated CFs produced by electroless nickel plating were the most effective conductive fillers for EMI shielding. Huang et al. [49,101] also studied the EMI shielding effectiveness of metal-coated CF-reinforced PC/ABS composites. The results indicated that the resistivity of the nickel-coated CF/ABS composites increased significantly after composite fabrication. The highest EMI shielding effectiveness obtained with the composites was 65 dBm.

4.2. PA-based composites

Wu et al. [52] studied the mechanical, thermal, and morphological properties of glass-fiber- and CF-reinforced PA6 and PA6/clay nanocomposites. Their results indicated that the mechanical and thermal properties of the PA6/clay nanocomposites were superior to those of the PA6 composite and there was no sacrifice of the impact strength. The heat distortion temperature of the CF-reinforced PA6/clay composites was almost 20 °C higher than that of the CF-reinforced PA6 composites. Yan et al. [58] studied the preparation and characterization of CF/PA12 composites for selective laser sintering. The CF/PA 12 composites exhibited higher thermal stability than pure PA12. The sintered CF/PA composites exhibited greatly enhanced flexural strength and flexural moduli compared with pure sintered PA12. Surface fracture analysis revealed that the CFs were encapsulated and bonded well with the PA12 matrix. Karsli et al. [54] investigated the tensile and thermo-mechanical properties of SCF-reinforced PA6 composites. Evaluation of the mechanical parameters indicated that the tensile strength, modulus, and hardness increased and the strain－at－break of the composites decreased with increasing CF content. Dynamic mechanical analysis (DMA) revealed that the storage modulus and loss modulus of the composites increased with increasing SCF content. Ma et al. [102] studied the failure behavior and mechanical properties of CF-reinforced PA6 laminates. Tensile strength analysis indicated that the CF/PA6 laminates exhibited step-like fracture in the interfacial fracture mode with weak interfaces.

Kurokawa et al. [53] investigated the gear performance of CF-reinforced PA12. Their results indicated that the composites exhibits excellent load-bearing characteristics when grease was present in the engagement region. The load-bearing capacity was enhanced by increasing the molecular weight of PA12. Botelho et al. [59] compared the mechanical behavior of CF-reinforced PA6 and PA66 composites. The elastic modulus, tensile strength, and compressive strength of the composite increased slightly with increasing CF content. Scanning electron microscopy (SEM) analysis revealed that damage to the composite occurred largely via shear failure at the fiber/matrix interface, where failure was initiated at relatively low stress. Hassan et al. [55] studied the structure–property relationship of injection-molded SCF-reinforced PA66 composites. Their results indicated that the tensile strength and tensile modulus of the composites increased with increasing CF content. Li [103] investigated the interfacial properties of O_3-treated CF-reinforced PA6 composites. A 60% augmentation of the interfacial shear strength (IFSS) of the composites was achieved with O_3-treated CF compared with the untreated counterparts. XPS analysis revealed that O_3 treatment increased the amount of carboxyl groups on the CF surface, thereby enhancing the interfacial adhesion between the CFs and PA6 matrix. Do et al. [18] studied the effect of PP on the mechanical properties and water absorption of CF-reinforced PA6/PP composites. The results indicated that the ultimate tensile strength, elastic modulus, elongation, density for weight reduction, and dimensional stability of the composites with PP exhibited were superior to those of the composite without PP.

Dickson et al. [61] investigated the influence of the fiber orientation, fiber type, and volume fraction on the mechanical properties of continuous CF-reinforced PA composites. The results indicated an up to 6.3-fold enhancement of the tensile strength of the composites compared with that of non-reinforced PA. Li et al. [62] studied the effects of the thermal histories on the interfacial properties of continuous CF/PA 6 composites. Their results revealed that the IFSS of the composites decreased at slower cooling rates and higher annealing temperatures.

4.3. PC-based composites

Carneiro et al. [104] prepared PC composites reinforced with vapor-grown CFs. The tensile properties of the injection-molded specimens were marginally better than those of the unreinforced PC; however, the impact resistance was severely diminished by the addition of CFs. Park [105] studied the interfacial properties of CF-reinforced PC composites using two types of coupling agents. It was found that both coupling agents caused an increase in the IFSS due to chemical and hydrogen bonding at the interface between the functional groups in the CFs and polyacrylamide in the coupling agents. Montes－Morán et al. [106] investigated the effects of plasma oxidation on the surface and interfacial properties of CF-reinforced PC composites. Plasma treatment significantly increased the interfacial shear strength of the CF/PC composites by increasing the number of surface functional groups. Hornbostel et al. [64] investigated the mechanical properties of triple composites of PC, single-walled carbon nanotubes (SWCNTs), and CFs. Small amounts of CNTs randomly distributed in the PC matrix did not necessarily enhance the mechanical stability, whereas greater mechanical improvements were attained by adding CFs to the composites.

Choi et al. [63] studied the electrical and mechanical properties of PC composite sheets reinforced with vapor-grown CFs. Microscopic analysis revealed a homogeneous dispersion of CFs in the PC matrix. The electrical resistivity of the CF/PC composites decreased with increasing CF loading because of the presence of a good fiber network. The mechanical properties of the composite improved greatly because of the enhanced fiber orientation. Ozkan et al. [66] investigated the effects of sizing materials on the mechanical, electrical, and morphological properties of SCF-reinforced PC composites. Their results indicated that the tensile strength, modulus, and electrical conductivity of

sized CF/PC composites were higher than those of unsized CF/PC composites. SEM analysis revealed better interactions between the phenoxy-sized CF and PC matrix.

4.4. PEEK-based composites

Hanchi et al. [70] investigated the effects of the operating temperature on the dry sliding friction and wear performance of a SCF-reinforced PEEK composite. The wear performance of the composite decreased when the temperatures was increased from below to above the T_g. In the sliding regime above the T_g, the friction and wear performance of the composite was significantly better than that of neat PEEK. Xie et al. [69] investigated the tribological behavior of a PEEK composite reinforced with CFs and potassium titanate whiskers (PTW) using a pin-on-disk configuration. Their results indicated that the CF/PTW/PEEK composite exhibited excellent tribological performance under aqueous conditions. The results also revealed that the two fillers worked synergistically to enhance the wear resistance of the composite.

Tewari et al. [107] characterized the solid particle erosion behavior of unidirectional CF-reinforced PEEK composites. The CF/PEEK composites exhibited semi-ductile erosion behavior. SEM observations indicated that the composites underwent erosion damage via matrix removal and exposure of the fibers, fiber cracking, and removal of broken fibers.

Almajid et al. [72] investigated the surface damage characteristics of continuous CF-reinforced PEEK composites under sliding and rolling contact. The composite with a normal fiber orientation exhibited the lowest specific wear rate under rolling wear conditions, whereas parallel fiber orientation resulted in the lowest specific wear rate in the case of sliding wear. Fujihara et al. [73] studied the effect of the processing conditions on the bend-ability of continuous CF-reinforced PEEK composites. It was found that the bending performance of the composites was significantly affected at 440 °C. A lower fabrication temperature and a shorter holding time were the most suitable processing conditions for preparation of the CF/PEEK composites.

4.5. PEI-based composites

Xian et al. [108] studied the tribological behavior of SCF/PEI composites using both a block-on-ring and pin-on-disc rig under dry sliding conditions. The coefficient of friction decreased and the wear resistance increased significantly with the addition of 5–20 vol% CFs. Sharma et al. [75] studied the effect of the orientation of long CFs on the mechanical and tribological properties of CF/PEI composites. It was found that the tribological properties of the composites deteriorated when the angle of orientation of the fibers in the composites increased from 0° to 90°. Sharma et al. [74] also examined the effect of the fiber orientation on the abrasive wear of CF/PEI composites. The Young's modulus, Poisson's ratio, toughness, and strain decreased when the angle of orientation of fiber with respect to the loading direction was higher. Unidirectional CF reinforcement significantly enhanced all the strength parameters of PEI.

Arjula et al. [109] investigated the erosive wear behavior of unidirectional CF-reinforced PEI composites. The investigated CF/PEI composites exhibited semi-ductile behavior in low-speed erosive studies. Higher particle speeds resulted in a rougher surface because of severe fiber breakage and matrix erosion. Arjula et al. [110] also studied the effect of the CF orientation on the erosion rate of CF/PEI composites, demonstrating that the rate of erosion of the CF/PEI composites was significantly higher than that of neat PEI at higher impact angles. The rate of erosion of the composite was higher for 90° orientation than for 0° orientation of the fibers.

4.6. PES-based composites

Yumitori et al. [78] studied the role of sizing resins in CF-reinforced PES. The sized CFs exhibited a higher interfacial shear strength than the unsized counterparts due to the strong interaction between the sizing resin in the CFs and the PES matrix. Wu et al. [79] investigated the processing and properties of solution-impregnated CF-reinforced PES composites, where the longitudinal flexural modulus and flexural strength were found to be 137 GPa and 1400 MPa, respectively. Their results also suggested that the transverse properties and interlaminar fracture toughness improved when the molecular weight of the polymer matrix was higher. Zheng et al. [77] blended PEI and PES to improve the rheological properties of a PPESK matrix and provide sufficient impregnation and consolidation during the hot-press molding treatment of CF/PPESK composites. The mechanical properties of the CF/PPESK/PEI and CF/PPESK/PES composites were markedly improved, which was attributed to the good interfacial adhesion and low porosity resulting from the addition of PEI and PES to the PPESK matrix. Li et al. [111] investigated the cryogenic mechanical properties of SCF/PES composites using a graphene oxide (GO) coating. The GO-coated SCF/PES composites displayed greatly enhanced cryogenic mechanical properties compared with the SCF/PES composites.

4.7. PE-based composites

Savas et al. [86] prepared CF-reinforced HDPE composites using PE copolymers as compatibilizers. Their results indicated that enhanced mechanical properties of the composites were achieved with all of the compatibilizers relative to the composites without compatibilizers. Chukov et al. [112] investigated the structural, mechanical, and tribological properties of SCF-reinforced ultra-high molecular weight PE (UHMWPE) composites. The results indicated that thermal oxidation of the CFs by ambient oxygen at 500 °C significantly enhanced the interfacial interaction between the CFs and polymer matrix. Their results also revealed that the yield stress of the composites was almost twice as higher as that of pure UHMWPE. Erkendirci et al. [113] studied the quasi−static penetration resistance behavior of CF-reinforced HDPE composites. These composites exhibited a large effective displacement for complete energy dissipation, where more energy was dissipated in the case of thinner laminates and less energy was dissipated for thicker composites.

Zhang et al. [82] studied the selective location and double−percolation of SCF-filled HDPE/isotactic PP (iPP) blends. The percolation threshold of the SCF-filled HDPE/iPP blends was found to be lower than those of the individual polymers. SEM analysis verified that the improvement in the electrical conductivity could be attributed to the selective location of the SCFs in the HDPE phase. Thongruang et al. [83] studied the correlation of the electrical conductivity and mechanical properties of HDPE filled with graphite and CFs. Their results indicated that the addition of CFs to the HDPE/graphite composites increased the conductivity relative to that of HDPE/graphite composites. Optical and electron micrographs revealed that the CFs exhibited preferential alignment depending on their length relative to the thickness of the composite film. Xi et al. [114] studied the dielectric effects on the positive temperature coefficient (PTC) of SCF/PE composites. An excellent PTC effect was achieved by adding SCFs to the PE matrix. The conductive CFs aggregated in series, where an equivalent circuit of a resistor and capacitor were arranged in parallel, representing the blends at these contact regions. Shen et al. [115] investigated the combined effects of carbon black (CB) and CFs on the electrical properties of composites based on PE or a PE/PP blend. The volume resistivities of the HDPE/CB/CF and HDPE/PP/CB/CF composites were lower than those of the HDPE/CB and HDPE/PP/CB composites, respectively. The intensity of the PTC and the temperature coefficient of resistivity of the HDPE/CB/CF and HDPE/PP/CB/CF composites increased appreciably with increasing CF loading.

4.8. PPS-based composites

Liu et al. [88] studied the interfacial micromechanical performance of CF-reinforced PPS composites using microbond analysis. The IFSS of the composites increased with the length of the embedded CFs at speeds below 0.02 mm/s and above 0.04 mm/s; however, the IFSS remained constant at speeds between 0.02 and 0.04 mm/s. Zhou et al. [89] investigated the effect of CFs on the structural, mechanical, and tribological properties of PA6/PPS composites. Introduction of the CFs resulted in an increase in the strength, modulus, and hardness and a slight decrease in the breaking elongation rate and impact strength of the PA6/PPS blends. SEM observation revealed that the main wear mechanism of the composites was adhesive wear. Stoeffler et al. [91] investigated the mechanical and physical properties of PPS composites reinforced with recycled CF. Their results indicated that the mechanical properties of recycled CF-reinforced PPS composites were equivalent to those of compounds produced using industrial grades of virgin CF. Thermogravimetric analysis (TGA) revealed that the introduction of recycled CFs was not detrimental to the inherent thermal stability of PPS. Zhang et al. [116] studied the effect of aminated PPS (PPS-NH_2) on the mechanical properties of SCF-reinforced PPS composites. Amination improved the compatibility between the CFs and PPS matrix. The tensile strength, flexural strength, and flexural modulus of the CF/PPS composites with compatibilizers were better than those of the composites without the compatibilizer because of the enhanced adhesion at the interface of the CFs and PPS-NH_2.

Xu et al. [117] investigated the tribological behavior of CF-reinforced PPS composite coatings under dry sliding and water lubricated conditions. The composite coatings exhibited lower friction coefficients and higher wear rates than the pure PPS coatings under dry sliding. The composite coatings exhibited better wear resistance with water-lubrication than under dry sliding conditions. Jiang et al. [90] studied the friction and wear behavior of PPS composites reinforced with SCFs and sub-micro TiO_2 particles. The lowest specific wear rate was obtained with 15 vol% CF and 5 vol% TiO_2. SEM analysis revealed a positive rolling effect of the particles between the two sliding surfaces, which protected the SCFs from being pulled out of the PPS matrix.

4.9. PP-based composites

Rezaei et al. [118] studied the effect of the length of CFs on the thermo-mechanical properties of SCF-reinforced PP composites. Their results suggested that longer CFs imparted better thermo-mechanical properties to the CF/PP composites than shorter CFs. TGA also indicated that the thermal stability of the SCF/PP composites increased with increasing CF length. Wang et al. [119] studied the mechanical and thermal properties of SCF-reinforced PP composites coated with GO. The tensile, flexural, and impact strengths of the GO-coated SCF/PP composites were greatly improved by the chemical reaction and mechanical interlocking between GO on the surface of the SCFs and the PP matrix. Differential scanning calorimetry (DSC) indicated that the GO-SCF/PP composites exhibited good thermal stability.

Fu et al. [120] investigated the fracture resistance of short-glass-fiber-reinforced and SCF-reinforced PP under Charpy impact load. The notched Charpy impact energy of the composites was found to increase with increasing glass fiber content and decreasing CF content. Han et al. [121] evaluated the surface treatment of CFs on the interfacial behavior of CF-reinforced PP composites. A 29.7% increase in the IFSS of the composites subjected to 3 min plasma treatment was achieved compared with that of the untreated specimens. The IFSS of the composites increased by 48.7% when treated with a silane coupling agent and subjected to 1 min plasma treatment compared with that of the untreated specimen. Karsli et al. [94] investigated the effects of an irradiated PP compatibilizer on the properties of SCF-reinforced PP composites. Their results indicated an increase in the breaking strength values to 30%. SEM observation indicated that enhanced interfacial adhesion between the CF and PP matrix was achieved in blends comprising the PP matrix and irradiated PP. Arao et al. [95] studied the mechanical properties of CF/PP composites hybridized with nanofillers. The IFSS and mechanical properties of the CF/PP composites improved with the addition of alumina, silica, and CNTs. The alumina particles were most effective for enhancing the mechanical properties of the composites.

Akonda et al. [122] studied recycled-CF-reinforced PP composites. The tensile and flexural strengths of the composites containing 27.7 vol % recycled CFs were 160 and 154 MPa, respectively. Wong et al. [123] investigated the effect of coupling agents on the potential of recycled CF as a reinforcement for PP composites. The interfacial adhesion was improved by the addition of maleic anhydride grafted polypropylene (MAPP). The impact strength of the composites improved significantly when MAPP was added due to greater compatibility between the CFs and matrix.

Ameli et al. [124] investigated the electrical properties and EMI shielding effectiveness of CF/PP composite foams. The density of the composites decreased by 25%, the through-plane conductivity was enhanced to a maximum of six orders of magnitude, and the dielectric permittivity increased, resulting in an increase in the specific EMI shielding effectiveness by up to 65% with the introduction of foaming. Zhao et al. [92] studied the effect of CFs on the conductive properties of a segregated CB/PP composite. The percolation threshold of the composite decreased significantly with the addition of 0.155 vol% CFs. Based on SEM analysis, the reduction of the percolation threshold was attributed to the construction of a shish-calabash-like conductive network. Hong et al. [96] investigated the EMI shielding effectiveness of CF-reinforced PP composites in the presence of CNTs as a conductive filler. The EMI shielding effectiveness of the CF/PP composites increased with increasing mixing speed due to the enhanced dispersion of the CFs in the matrix, which resulted in improvement of the electrical networks, and thus the EMI shielding effectiveness, in the CF/PP composites. Xu et al. [125] studied the liquid sensing behavior of conductive PP composites containing CFs and CB. The CF/CB/PP composite exhibited superior liquid sensing behavior compared with the CB/PP composite.

Cho et al. [98] achieved highly enhanced mechanical properties of long CF-reinforced PP composites by a combined method involving a coupling agent and surface modification of CFs. The surface−modified CF-reinforced PP composite with 5 wt% bi-functional group-grafted PP as a coupling agent showed the highest tensile strength and flexural strength, with respective increases of 1.5- and 1.7-fold respectively, compared with the PP/CF composite employing conventional maleic anhydride-grafted PP. Hou et al. [99] determined the processing conditions, such as stamping temperature, stamping time, stamping velocity, and pressure required for stamp forming of continuous CF-reinforced PP composites. An experimental two-dimensional matched die was successfully designed and employed for stamp-forming of continuous CF-reinforced PP composites.

4.10. Advantages and disadvantages of CFs in thermoplastic composites

The advantages of using CFs in thermoplastic composites are as follows [18,19,75,86,126,127]:

1. As advanced reinforcing fiber materials in thermoplastic composites, CFs have excellent mechanical, thermal, and electrical properties, good thermal conductivity, excellent corrosion resistance, a low linear thermal expansion coefficient, and low density.
2. Compared to short glass fibers, SCFs have low density, high specific strength and stiffness, excellent thermal and electrical conductivity, high wear resistance, and a low coefficient of friction, making them attractive for many applications, especially in the automotive industry.
3. Continuous CF-reinforced thermoplastic composites have been

extensively used in the aerospace, weaponry, automotive, and chemical industries because of their potential for construction of lightweight materials, high strength and stiffness, recyclability, repairability, and corrosion resistance.
4. CF-reinforced thermoplastics can be recycled by melting the material and reforming it into a new object.

The disadvantages of the use of CFs in thermoplastic composites are as follows [26,112,128,129]:

1. CFs are expensive compared with glass fibers.
2. CFs have poor wettability and adhesion to the thermoplastic matrix.
3. Unidirectional CF-reinforced thermoplastic composites exhibit low strain under uniaxial tension.

4.11. Problems with CF-reinforced thermoplastic composites and possible solutions

4.11.1. High cost of CFs compared with glass fibers

To obtain thermoplastics reinforced with SCFs, composites can be prepared by using recycled CFs. These fibers are much cheaper than the initial CFs and can be used to reinforce thermoplastic polymers in order to improve their physical, mechanical, tribological, thermal, and electrical properties [112].

4.11.2. Poor wettability and adhesion of CFs to the thermoplastic matrix

The surfaces of CFs can treated using chemical methods, plasma methods, electrochemical methods, and sizing or coating methods to introduce chemical functional groups onto the fiber surface and improve the interfacial adhesion between the CFs and the thermoplastic matrix [128].

4.11.3. Low strain of unidirectional CF-reinforced thermoplastic composites under uniaxial tension

In order to increase the strain to tensile failure, different techniques such as thin-ply hybridization, thin-ply CF-reinforced plastic angle ply lamination, wavy-ply sandwich structures, and interleaved lamination can be employed [129].

4.11.4. Negative influence of residual solvent in the solution-processed system on the performance of CF-reinforced thermoplastic composites

In solution-processed systems, CF-reinforced thermoplastic composite prepregs can be fabricated by impregnating CFs with a suitable polymer solution. This process can lower the viscosity of the resulting polymer solution and thus reduce the processing cost. However, the residual solvent may influence the performance of the composites. The residual solvent in solution-processed products should be removed by employing a higher molding temperature and/or longer molding time [75].

5. Conclusion

This review covered the recent advances in methods of surface treatment of CFs and preparation of CF/thermoplastic composites. Suitable surface treatments and preparation methods are important for achieving a uniform dispersion of CFs in polymer matrices and for increasing the interfacial adhesion between the CFs and matrix. Furthermore, the thermal, mechanical, and electrical properties of the composites were discussed in detail. Recent studies have focused on the preparation and characterization of nanoparticle-filled CF/thermoplastic composites as a means of achieving significantly improved mechanical and electrical properties.

Appendix A. Supplementary data

Supplementary data related to this article can be found at http://dx.doi.org/10.1016/j.compositesb.2017.12.007.

References

[1] Park SJ, Seo MK. Carbon fiber-reinforced polymer composites: preparation, properties, and applications. Polymer composites, vol. 1. Germany: Wiley-VCH Verlag GmbH & Co. KGaA, Weinheim; 2012.
[2] Park SJ, Lee SY, Jin FL. Surface modification of carbon nanotubes for high-performance polymer composites. Handbook of polymer nanocomposites, B. Springer; 2015.
[3] Kim M, Sung DH, Kong K, Kim N, Kim BJ, Park HW, et al. Characterization of resistive heating and thermoelectric behavior of discontinuous carbon fiber-epoxy composites. Compos Part B 2016;90:37–44.
[4] Xu H, Zhang X, Liu D, Yan C, Chen X, Hui D, et al. Cyclomatrix-type polyphosphazene coating: improving interfacial property of carbon fiber/epoxy composites and preserving fiber tensile strength. Compos Part B 2016;93:244–51.
[5] Wang FS, Ji YY, Yu XS, Chen H, Yue ZF. Ablation damage assessment of aircraft carbon fiber/epoxy composite and its protection structures suffered from lightning strike. Compos Struct 2016;145:226–41.
[6] Dawood M, El-Tahan MW, Zheng B. Bond behavior of superelastic shape memory alloys to carbon fiber reinforced polymer composites. Compos Part B 2015;77:238–47.
[7] Chowdhury NM, Chiu WK, Wang J, Chang P. Experimental and finite element studies of bolted, bonded and hybrid step lap joints of thick carbon fibre/epoxy panels used in aircraft structures. Compos Part B 2016;100:68–77.
[8] Lu JH, Youngblood JP. Adhesive bonding of carbon fiber reinforced composite using UV-curing epoxy resin. Compos Part B 2015;82:221–5.
[9] Yamamoto T, Uematsu K, Irisawa T, Tanabe Y. Controlling of the interfacial shear strength between thermoplastic resin and carbon fiber by adsorbing polymer particles on carbon fiber using electrophoresis. Compos Part A 2016;88:75–8.
[10] Dhieb H, Buijnsters JG, Elleuch K, Celis JP. Effect of relative humidity and full immersion in water on friction, wear and debonding of unidirectional carbon fiber reinforced epoxy under reciprocating sliding. Compos Part B 2016;88:240–52.
[11] Hwang S. Tensile, electrical conductivity and EMI shielding properties of solid and foamed PBT/carbon fiber composites. Compos Part B 2016;98:1–8.
[12] Ning F, Cong W, Qiu J, Wei J, Wang S. Additive manufacturing of carbon fiber reinforced thermoplastic composites using fused deposition modeling. Compos Part B 2015;80:269–78.
[13] Jin FL, Lee SY, Park SJ. Polymer matrices for carbon fiber-reinforced polymer composites. Carbohydr Lett 2013;14:76–88.
[14] Zhao YH, Zhang YF, Bai SL, Yuan XW. Carbon fibre/graphene foam/polymer composites with enhanced mechanical and thermal properties. Compos Part B 2016;94:102–8.
[15] Hong S, Park SK. Effect of prestress and transverse grooves on reinforced concrete beams prestressed with near-surface-mounted carbon fiber-reinforced polymer plates. Compos Part B 2016;91:640–50.
[16] Jin FL, Park SJ. Preparation and characterization of carbon fiber-reinforced thermosetting composites: a review. Carbohydr Lett 2015;16:67–77.
[17] Gabrion X, Placet V, Trivaudey F, Boubakar L. About the thermomechanical behaviour of a carbon fibre reinforced high-temperature thermoplastic composite. Compos Part B 2016;95:386–94.
[18] Do VT, Nguyen-Tran HD, Chun DM. Effect of polypropylene on the mechanical properties and water absorption of carbon-fiber-reinforced-polyamide-6/polypropylene composite. Compos Struct 2016;150:240–5.
[19] Luo W, Liu Q, Li Y, Zhou S, Zou H, Liang M. Enhanced mechanical and tribological properties in polyphenylene sulfide/polytetrafluoroethylene composites reinforced by short carbon fiber. Compos Part B 2016;91:579–88.
[20] Wu G, Ma L, Liu L, Wang Y, Xie F, Zhong Z, et al. Interfacially reinforced methylphenylsilicone resin composites by chemically grafting multiwall carbon nanotubes onto carbon fibers. Compos Part B 2015;82:50–8.
[21] Park SJ, Jang YS, Kawasaki J. Studies on nanoscaled Ni-P plating of carbon fiber surfaces in a composite system. Carbohydr Lett 2002;3:77–9.
[22] Lee HS, Kim S, Noh YJ, Kim SY. Design of microwave plasma and enhanced mechanical properties of thermoplastic composites reinforced with microwave plasma-treated carbon fiber fabric. Compos Part B 2014;60:621–6.
[23] Nagura Azusa, Okamoto Kazuaki, Itoh Kiyoharu, Imai Yusuke, Shimamoto Daisuke, Hotta Yuji. The Ni-plated carbon fiber as a tracer for observation of the fiber orientation in the carbon fiber reinforced plastic with X-ray CT. Compos Part B 2015;76:38–43.
[24] Park SJ, Jang YS, Shim JW, Ryu SK. Studies on pore structures and surface functional groups of pitch-based activated carbon fibers. J Colloid Interface Sci 2003;260:259–64.
[25] Shin HK, Park M, Kim HY, Park SJ. An overview of new oxidation methods for polyacrylonitrile-based carbon fibers. Carbohydr Lett 2015;16:11–8.
[26] Bachinger A, Rössler J, Asp LE. Electrocoating of carbon fibres at ambient conditions. Compos Part B 2016;91:94–102.
[27] Park SJ, Seo MK, Lee YS. Surface characteristics of fluorine-modified PAN-based carbon fibers. Carbon 2003;41:723–30.
[28] Park SJ, Park BJ. Electrochemically modified PAN carbon fibers and interfacial adhesion in epoxy-resin composites. J Mater Sci Lett 1999;18:47–9.
[29] Zhang G, Sun S, Yang D, Dodelet JP, Sacher E. The surface analytical characterization of carbon fibers functionalized by H_2SO_4/HNO_3 treatment. Carbon 2008;46:196–205.
[30] Wu Z, Pittman CU. Nitric acid oxidation of carbon fibers and the effects of subsequent treatment in refluxing aqueous NaOH. Carbon 1995;33:597–605.

[31] Ryu SK, Park BJ, Park SJ. XPS analysis of carbon fiber surfaces—anodized and interfacial effects in fiber–epoxy composites. J Colloid Interface Sci 1999;215:167–9.
[32] Seo MK, Park SJ. Surface characteristics of carbon fibers modified by direct oxyfluorination. J Colloid Interface Sci 2009;330:237–42.
[33] Park SJ, Seo MK, Lee JR. Relationship between surface characteristics and interlaminar shear strength of oxyfluorinated carbon fibers in a composite system. J Colloid Interface Sci 2003;268:127–32.
[34] Park SJ, Seo MK, Rhee KY. Studies on mechanical interfacial properties of oxyfluorinated carbon fibers-reinforced composites. Mater Sci Eng 2003;356:219–26.
[35] Park SJ, Seo MK, Lee YS. Surface and mechanical interfacial properties of oxyfluorinated carbon fibers-reinforced composites. Carbohydr Lett 2003;4:69–73.
[36] Park SJ, Kim MH, Lee JR, Choi S. Effect of fiber–polymer interactions on fracture toughness behavior of carbon fiber-reinforced epoxy matrix composites. J Colloid Interface Sci 2000;228:287–91.
[37] Park SJ, Donnet JB. Anodic surface treatment on carbon Fibers: determination of acid-base interaction parameter between two unidentical solid surfaces in a composite system. J Colloid Interface Sci 1998;206:29–32.
[38] Osbeck S, Bradley RH, Liu C, Idriss H, Ward S. Effect of an ultraviolet/ozone treatment on the surface texture and functional groups on polyacrylonitrile carbon fibres. Carbon 2011;49:4322–30.
[39] Park SJ, Kim BJ. Roles of acidic functional, groups of carbon fiber surfaces in enhancing interfacial adhesion behavior. Mater Sci Eng 2005;408:269–73.
[40] Zhang X, Huang Y, Wang T, Liu L. Influence of fibre surface oxidation–reduction followed by silsesquioxane coating treatment on interfacial mechanical properties of carbon fibre/polyarylacetylene composites. Compos Part A 2007;38:936–44.
[41] Iwashita N, Psomiadou E, Sawada Y. Effect of coupling treatment of carbon fiber surface on mechanical properties of carbon fiber reinforced carbon composites. Compos Part A 1998;29:965–72.
[42] Park SJ, Jang YS. X-ray diffraction and X-ray photoelectron spectroscopy studies of Ni–P deposited onto carbon fiber surfaces: impact properties of a carbon-fiber-reinforced matrix. J Colloid Interface Sci 2003;263:170–6.
[43] Park SJ, Jang YS. Interfacial characteristics and fracture toughness of electrolytically Ni-plated carbon fiber-reinforced phenolic resin matrix composites. J Colloid Interface Sci 2001;237:91–7.
[44] Park SJ, Jang YS, Rhee KY. Interlaminar and ductile characteristics of carbon fibers-reinforced plastics produced by nanoscaled electroless nickel plating on carbon fiber surfaces. J Colloid Interface Sci 2002;245:383–90.
[45] Park SJ, Kim BJ. Effect of Ni plating on mechanical interfacial properties of carbon fibers-reinforced composites. Carbohydr Lett 2002;3:152–4.
[46] Lu G, Li X, Jiang H. Electrical and shielding properties of ABS resin filled with nickel-coated carbon fibers. Compos Sci Technol 1996;56:193–200.
[47] Liang X, Ling L, Lu C, Liu L. Resistivity of carbon fibers/ABS resin composites. Mater Lett 2000;43:144–7.
[48] Tzeng SS, Chang FY. EMI shielding effectiveness of metal-coated carbon fiber-reinforced ABS composites. Mater Sci Eng 2001;302:258–67.
[49] Huang CY, Wu CC. The EMI shielding effectiveness of PC/ABS/nickel-coated-carbon-fibre composites. Eur Polym J 2000;36:2729–37.
[50] Huang CY, Pai JF. Optimum conditions of electroless nickel plating on carbon fibers for EMI shielding effectiveness of ENCF/ABS composites. Eur Polym J 1998;34:261–7.
[51] Li J, Cai CL. The carbon fiber surface treatment and addition of PA6 on tensile properties of ABS composites. Curr Appl Phys 2011;11:50–4.
[52] Wu SH, Wang FY, Ma CCM, Chang WC, Kuo CT, Kuan HC, et al. Mechanical, thermal and morphological properties of glass fiber and carbon fiber reinforced polyamide-6 and polyamide-6/clay nanocomposites. Mater Lett 2001;49:327–33.
[53] Kurokawa M, Uchiyama Y, Iwai T, Nagai S. Performance of plastic gear made of carbon fiber reinforced polyamide 12. Wear 2003;254:468–73.
[54] Karsli NG, Aytac A. Tensile and thermomechanical properties of short carbon fiber reinforced polyamide 6 composites. Compos Part B 2013;51:270–5.
[55] Hassan A, Hornsby PR, Folkes MJ. Structure–property relationship of injection-molded carbon fibre-reinforced polyamide 6,6 composites: the effect of compounding routes. Polym Test 2003;22:185–9.
[56] Yan X, Imai Y, Shimamoto D, Hotta Y. Relationship study between crystal structure and thermal/mechanical properties of polyamide 6 reinforced and unreinforced by carbon fiber from macro and local view. Polymer 2014;55:6186–94.
[57] Yoo Y, Lee HL, Ha SM, Jeon BK, Won JC, Lee SG. Effect of graphite and carbon fiber contents on the morphology and properties of thermally conductive composites based on polyamide 6. Polym Int 2014;63:151–7.
[58] Yan C, Hao L, Xu L, Shi Y. Preparation, characterisation and processing of carbon fibre/polyamide-12 composites for selective laser sintering. Compos Sci Technol 2011;71:1834–41.
[59] Botelho EC, Figiel L, Rezende MC, Lauke B. Mechanical behavior of carbon fiber reinforced polyamide composites. Compos Sci Technol 2003;63:1843–55.
[60] Luo H, Xiong G, Ma C, Li D, Wan Y. Preparation and performance of long carbon fiber reinforced polyamide 6 composites injection-molded from core/shell structured pellets. Mater Des 2014;64:294–300.
[61] Dickson AN, Barry JN, McDonnell KA, Dowling DP. Fabrication of continuous carbon, glass and Kevlar fibre reinforced polymer composites using additive manufacturing. Addit Manuf 2017;16:146–52.
[62] Li H, Wang Y, Zhang C, Zhang B. Effects of thermal histories on interfacial properties of carbon fiber/polyamide 6 composites: Thickness, modulus, adhesion and shear strength. Compos Part A 2016;85:31–9.
[63] Choi YK, Sugimoto K, Song SM, Endo M. Production and characterization of polycarbonate composite sheets reinforced with vapor grown carbon fiber. Compos Part A 2006;37:1944–51.
[64] Hornbostel B, Pötschke P, Kotz J, Roth S. Mechanical properties of triple composites of polycarbonate, single-walled carbon nanotubes and carbon fibres. Physica 2008;40:2434–9.
[65] Law TT, Phua YJ, Senawi R, Hassan A, Mohd Ishak ZA. Experimental analysis and theoretical modeling of the mechanical behavior of short glass fiber and short carbon fiber reinforced polycarbonate hybrid composites. Polym Compos 2016;37:1238–48.
[66] Ozkan C, Karsli NG, Aytac A, Deniz V. Short carbon fiber reinforced polycarbonate composites: Effects of different sizing materials. Compos Part B 2014;62:230–5.
[67] Zhang G, Latour RA, Kennedy JM, Schutte HD, Friedman RJ. Long-term compressive property durability of carbon fibre-reinforced polyetheretherketone composite in physiological saline. Biomaterials 1996;17:781–9.
[68] Luo H, Xiong G, Ren K, Raman SR, Liu Z, Li Q, et al. Air DBD plasma treatment on three-dimensional braided carbon fiber-reinforced PEEK composites for enhancement of in vitro bioactivity. Surf Coating Technol 2014;242:1–7.
[69] Xie GY, Sui GX, Yang R. Effects of potassium titanate whiskers and carbon fibers on the wear behavior of polyetheretherketone composite under water lubricated condition. Compos Sci Technol 2011;71:828–35.
[70] Hanchi J, Eiss NS. Dry sliding friction and wear of short carbon-fiber-reinforced polyetheretherketone (PEEK) at elevated temperatures. Wear 1997;203–204:380–6.
[71] Xu A, Liu X, Gao X, Deng F, Deng Y, Wei S. Enhancement of osteogenesis on micro/nano-topographical carbon fiber-reinforced polyetheretherketone-nanohydroxyapatite biocomposite. Mater Sci Eng C 2015;48:592–8.
[72] Almajid A, Friedrich K, Floeck J, Burkhart T. Surface damage characteristics and specific wear rates of a new continuous carbon fiber (CF)/polyetheretherketone (PEEK) composite under sliding and rolling contact conditions. Appl Compos Mater 2011;18:211–30.
[73] Fujihara K, Huang ZM, Ramakrishna S, Hamada H. Influence of processing conditions on bending property of continuous carbon fiber reinforced PEEK composites. Compos Sci Technol 2004;64:2525–34.
[74] Sharma M, Rao IM, Bijwe J. Influence of fiber orientation on abrasive wear of unidirectionally reinforced carbon fiber–polyetherimide composites. Tribol Int 2010;43:959–64.
[75] Sharma M, Rao IM, Bijwe J. Influence of orientation of long fibers in carbon fiber-polyetherimide composites on mechanical and tribological properties. Wear 2009;267:839–45.
[76] Xian G, Zhan Z. Sliding wear of polyetherimide matrix composites I. Influence of short carbon fibre reinforcement. Wear 2005;258:776–82.
[77] Zheng L, Liao GX, Gu TS, Han YJ, Jian XG. Modified continuous carbon fiber-reinforced poly(phthalazinone ether sulfone ketone) composites by blending polyetherimide and polyethersulfone. Polym Compos 2009;30:1842–7.
[78] Yumitori S, Wang D, Jones FR. The role of sizing resins in carbon fibre-reinforced polyethersulfone (PES). Composites 1994;25:698–705.
[79] Wu GM, Schultz JM. Processing and properties of solution impregnated carbon fiber reinforced polyethersulfone composites. Polym Compos 2000;21:223–30.
[80] Sengur R, Lannoy CF, Turken T, Wiesner M, Koyuncu I. Fabrication and characterization of hydroxylated and carboxylated multiwalled carbon nanotube/polyethersulfone (PES) nanocomposite hollow fiber membranes. Desalination 2015;359:123–40.
[81] Li F, Liu Y, Qu CB, Xiao HM, Hua Y, Sui GX, et al. Enhanced mechanical properties of short carbon fiber reinforced polyethersulfone composites by graphene oxide coating. Polymer 2015;59:155–65.
[82] Zhang C, Yi XS, Yui H, Asai S, Sumita M. Selective location and double percolation of short carbon fiber filled polymer blends: high-density polyethylene/isotactic polypropylene. Mater Lett 1998;36:186–90.
[83] Thongruang W, Spontak RJ, Balik CM. Correlated electrical conductivity and mechanical property analysis of high-density polyethylene filled with graphite and carbon fiber. Polymer 2002;43:2279–86.
[84] Li S, Li D. Carbon fiber reinforced highly filled charcoal powder/ultrahigh molecular weight polyethylene composites. Mater Lett 2014;134:99–102.
[85] Stepashkin AA, Chukov DI, Gorshenkov MV, Tcherdyntsev VV, Kaloshkin SD. Electron microscopy investigation of interface between carbon fiber and ultra high molecular weight polyethylene. J Alloy Comp 2014;586:S168–72.
[86] Savas LA, Tayfun U, Dogan M. The use of polyethylene copolymers as compatibilizers in carbon fiber reinforced high density polyethylene composites. Compos Part B 2016;99:188–95.
[87] Khan SM, Gull N, Munawar MA, Islam A, Zia S, Shafiq M, et al. 2D carbon fiber reinforced high density polyethylene multi-layered laminated composite panels: structural, mechanical, thermal and morphological profile. J Mater Sci Technol 2016;32:1077–82.
[88] Liu B, Liu Z, Wang X, Zhang G, Long S, Yang J. Interfacial shear strength of carbon fiber reinforced polyphenylene sulfide measured by the microbond test. Polym Test 2013;32:724–30.
[89] Zhou S, Zhang Q, Wu C, Huang J. Effect of carbon fiber reinforcement on the mechanical and tribological properties of polyamide6/polyphenylene sulfide composites. Mater Des 2013;44:493–9.
[90] Jiang Z, Gyurova LA, Schlarb AK, Friedrich K, Zhang Z. Study on friction and wear behavior of polyphenylene sulfide composites reinforced by short carbon fibers and sub-micro TiO_2 particles. Compos Sci Technol 2008;68:734–42.
[91] Stoeffler K, Andjelic S, Legros N, Roberge J, Schougaard SB. Polyphenylene sulfide (PPS) composites reinforced with recycled carbon fiber. Compos Sci Technol 2013;84:65–71.
[92] Zhao S, Zhao H, Li G, Dai K, Zheng G, Liu C, et al. Synergistic effect of carbon fibers on the conductive properties of a segregated carbon black/polypropylene composite. Mater Lett 2014;129:72–5.

[93] Unterweger C, Duchoslav J, Stifter D, Fürst C. Characterization of carbon fiber surfaces and their impact on the mechanical properties of short carbon fiber reinforced polypropylene composites. Compos Sci Technol 2015;108:41–7.
[94] Karsli NG, Aytac A, Akbulut M, Deniz V, Güven O. Effects of irradiated polypropylene compatibilizer on the properties of short carbon fiber reinforced polypropylene composites. Radiat Phys Chem 2013;84:74–8.
[95] Arao Y, Yumitori S, Suzuki H, Tanaka T, Tanaka K, Katayama T. Mechanical properties of injection-molded carbon fiber/polypropylene composites hybridized with nanofillers. Compos Part A 2013;55:19–26.
[96] Hong MS, Choi WK, An KH, Kang SJ, Park SJ, Lee YS, et al. Electromagnetic interference shielding behaviors of carbon fibers-reinforced polypropylene matrix composites: II. Effects of filler length control. J Ind Eng Chem 2014;20:3901–4.
[97] Gabr MH, Okumura W, Ueda H, Kuriyama W, Uzawa K, Kimpara I. Mechanical and thermal properties of carbon fiber/polypropylene composite filled with nano-clay. Compos Part B 2015;69:94–100.
[98] Cho SM, Jung HT. Highly enhanced mechanical properties of polypropylene-long carbon fiber composites by a combined method of coupling agent and surface modification of long carbon fiber. Macromol Res 2014;22:1066–73.
[99] Hou M, Friedrich K. Stamp forming of continuous carbon fibre/polypropylene composites. Compos Manuf 1991;2:3–9.
[100] Li J, Zhang YF. The tensile properties of HNO_3-treated carbon fiber reinforced ABS/PA6 composites. Surf Interface Anal 2009;41:610–4.
[101] Huang CY, Mo WW, Roan ML. Studies on the influence of double-layer electroless metal deposition on the electromagnetic interference shielding effectiveness of carbon fiber/ABS composites. Surf Coating Technol 2004;184:163–9.
[102] Ma Y, Yang Y, Sugahara T, Hamada H. A study on the failure behavior and mechanical properties of unidirectional fiber reinforced thermosetting and thermoplastic composites. Compos Part B 2016;99:162–72.
[103] Li J. Interfacial studies on the O_3 modified carbon fiber-reinforced polyamide 6 composites. Appl Surf Sci 2008;255:2822–4.
[104] Carneiro OS, Covas JA, Bernardo CA, Caldeira G, Van Hattum FWJ, Ting JM, et al. Production and assessment of polycarbonate composites reinforced with vapour-grown carbon fibres. Compos Sci Technol 1998;58:401–7.
[105] Park JM. Interfacial properties of two CF-reinforced polycarbonate composites using two-synthesized graft copolymers as coupling agents. J Colloid Interface Sci 2000;225:384–93.
[106] Montes-Morán MA, Martínez-Alonso A, Tascón JMD, Paiva MC, Bernardo CA. Effects of plasma oxidation on the surface and interfacial properties of carbon fibres/polycarbonate composites. Carbon 2001;39:1057–68.
[107] Tewari US, Harsha AP, Häger AM, Friedrich K. Solid particle erosion of unidirectional carbon fibre reinforced polyetheretherketone composites. Wear 2002;252:992–1000.
[108] Xian G, Zhang Z. Sliding wear of polyetherimide matrix composites I. Influence of short carbon fibre reinforcement. Wear 2005;258:776–82.
[109] Arjula S, Sınmazçelik T. Erosive wear behaviour of carbon fibre/polyetherimide composites under low particle speed. Mater Des 2007;28:351–5.
[110] Arjula S, Harsha AP, Ghosh MK. Erosive wear of unidirectional carbon fibre reinforced polyetherimide composite. Mater Lett 2008;62:3246–9.
[111] Li F, Hua Y, Qu CB, Xiao HM, Fu SY. Greatly enhanced cryogenic mechanical properties of short carbon fiber/polyethersulfone composites by graphene oxide coating. Compos Part A 2016;89:47–55.
[112] Chukov DI, Stepashkin AA, Maksimkin AV, Tcherdyntsev VV, Kaloshkin SD, Kuskov KV, et al. Investigation of structure, mechanical and tribological properties of short carbon fiber reinforced UHMWPE-matrix composites. Compos Part B 2015;76:79–88.
[113] Erkendirci OF. Investigation of the quasi static penetration resistance behavior of carbon fiber reinforced laminate HDPE composites. Compos Part B 2016;93:344–51.
[114] Xi Y, Bin Y, Chiang CK, Matsuo M. Dielectric effects on positive temperature coefficient composites of polyethylene and short carbon fibers. Carbon 2007;45:1302–9.
[115] Shen L, Wang FQ, Yang H, Meng QR. The combined effects of carbon black and carbon fiber on the electrical properties of composites based on polyethylene or polyethylene/polypropylene blend. Polym Test 2011;30:442–8.
[116] Zhang K, Zhang G, Liu B, Wang X, Long S, Yang J. Effect of aminated polyphenylene sulfide on the mechanical properties of short carbon fiber reinforced polyphenylene sulfide composites. Compos Sci Technol 2014;98:57–63.
[117] Xu H, Feng Z, Chen J, Zhou H. Tribological behavior of the carbon fiber reinforced polyphenylene sulfide (PPS) composite coating under dry sliding and water lubrication. Mater Sci Eng 2006;416:66–73.
[118] Rezaei F, Yunus R, Ibrahim NA. Effect of fiber length on thermomechanical properties of short carbon fiber reinforced polypropylene composites. Mater Des 2009;30:260–3.
[119] Wang CC, Zhao YY, Ge HY, Qian RS. Enhanced mechanical and thermal properties of short carbon fiber reinforced polypropylene composites by graphene oxide. Polym Compos 2016.
[120] Fu SY, Lauke B, MaÈder E, Hu X, Yue CY. Fracture resistance of short-glass-fiber-reinforced and short-carbon-fiber-reinforced polypropylene under Charpy impact load and its dependence on processing. J Mater Process Technol 1999;89–90:501–7.
[121] Han SH, Oh HJ, Kim SS. Evaluation of fiber surface treatment on the interfacial behavior of carbon fiber-reinforced polypropylene composites. Compos Part B 2014;60:98–105.
[122] Akonda MH, Lawrence CA, Weager BM. Recycled carbon fibre-reinforced polypropylene thermoplastic composites. Compos Part A 2012;43:79–86.
[123] Wong KH, Mohammed SD, Pickering SJ, Brooks R. Effect of coupling agents on reinforcing potential of recycled carbon fibre for polypropylene composite. Compos Sci Technol 2012;72:835–44.
[124] Ameli A, Jung PU, Park CB. Electrical properties and electromagnetic interference shielding effectiveness of polypropylene/carbon fiber composite foams. Carbon 2013;60:379–91.
[125] Xu Z, Wang N, Li N, Zheng G, Dai K, Liu C, et al. Liquid sensing behaviors of conductive polypropylene composites containing hybrid fillers of carbon fiber and carbon black. Compos Part B 2016;94:45–51.
[126] Kada D, Koubaa A, Tabak G, Migneault S, Garnier B, Boudenne A. Tensile properties, thermal conductivity, and thermal stability of short carbon fiber reinforced polypropylene composites. Polym Compos 2016.
[127] Nagura A, Okamoto K, Itoh K, Imai Y, Shimamoto D, Hotta Y. The Ni-plated carbon fiber as a tracer for observation of the fiber orientation in the carbon fiber reinforced plastic with X-ray CT. Compos Part B 2015;76:38–43.
[128] Duchoslav J, Unterweger C, Steinberger R, Fürst C, Stifter D. Investigation on the thermo-oxidative stability of carbon fiber sizings for application in thermoplastic composites. Polym Degrad Stabil 2016;125:33–42.
[129] Diao H, Robinson P, Wisnom MR, Bismarck A. Unidirectional carbon fibre reinforced polyamide-12 composites with enhanced strain to tensile failure by introducing fibre waviness. Compos Part A 2016;87:186–93.